ELSEVIER

Catalysis Today 53 (1999) 725–737

CATALYSIS TODAY

www.elsevier.com/locate/cattod

Catalytic decomposition of nitrous oxide over calcined cobalt aluminum hydrotalcites

S. Kannan [a,*], C.S. Swamy [b]

[a] *Silicates and Catalysis Discipline, Central Salt and Marine Chemicals Research Institute, Bhavnagar 364 002, India*
[b] *Department of Chemistry, Indian Institute of Technology, Chennai 600 036, India*

Abstract

Catalytic decomposition of nitrous oxide has been carried out over calcined cobalt aluminum hydrotalcites of general formula $[Co_{1-x}Al_x(OH)_2[CO_3]_{x/2}\ H_2O$ where $x = 0.25$–0.33 at 50 Torr (1 Torr = 133 Pa) initial pressure of N_2O in a static glass recirculatory reactor (130 cc) in the temperature range 150–280°C. All catalysts showed a first order dependence in N_2O without significant oxygen inhibition. The activity increased with an increase in cobalt concentration present in the sample. The catalyst precursor synthesized under low supersaturation (LS) exhibited a higher activity than the precursor synthesized by sequential precipitation (SP) method. The observed trend in the activity is explained based on the surface concentration of cobalt, determined by XPS and matrix effects. Prior to catalytic studies, the fresh and calcined samples were characterized by various physicochemical techniques such as XRD, FT–IR, TG–DSC, TEM (with EDAX) and BET surface area measurements.
©1999 Elsevier Science B.V. All rights reserved.

Keywords: Nitrous oxide decomposition; Hydrotalcite-like compounds; X-ray photoelectron spectroscopy; Mixed metal oxide

1. Introduction

Nitrous oxide is an environmental pollutant, owing to its potential involvement in stratospheric destruction of ozone layer and being a greenhouse gas [1]. The continuous increase in its concentration, both due to natural and anthropogenic sources (0.2–0.3% p/a) and longer atmospheric residence time (150 years), enforce us to develop efficient catalysts for its decomposition (into nitrogen and oxygen) to protect our global environment. Hydrotalcite-like (HT-like) compounds are a new class of layered materials, otherwise referred as anionic clays or layered double hydroxides, are receiving an increasing attention, especially for the synthesis of multicomponent catalysts [2]. Structurally, they possess positively charged brucite-like layers $[M(II)_{1-x}M(III)_x(OH)_2]$ with the interlayer space filled with anions and water molecules $[A^{n-}_{x/n}]\cdot mH_2O$ [3]. Calcination of these materials (>300°C) yield mixed metal oxides with unusual properties such as non-stoichiometry, high thermal stability and good surface area, which have been efficiently exploited for various catalytic transformations [4–10]. The results of our previous study [11] on the catalytic decomposition of nitrous oxide indicated that calcined cobalt aluminum hydrotalcites are more active than the claimed zeolite-based catalysts. In this paper, we would like to disclose the effect of synthetic methodology and cobalt concentration on the catalytic activity of these compounds An attempt has also been made to unravel the nature of active species participating in the reaction through

* Corresponding author. Tel.: +91-278-567-760; fax: +91-278-566970
E-mail address: salt@bhavnagar.com (S. Kannan)

0920-5861/99/$ – see front matter ©1999 Elsevier Science B.V. All rights reserved.
PII: S0920-5861(99)00159-5

X-ray diffraction (XRD) and X-ray photoelectron spectroscopy (XPS) studies.

2. Experimental

The samples were synthesized by sequential and low supersaturation methods. In sequential precipitation method, the precipitants namely $NaOH/Na_2CO_3$ were added to metal nitrate solution of appropriate concentration with an increasing pH under stirring at ambient temperature. In low supersaturation technique, both metal nitrates and precipitants were added slowly and simultaneously by holding the pH around 9–10. In both cases, the final pH was adjusted to 10. The samples were subjected to further aging wherein sequentially precipitated sample was treated at 65°C for 24 h without stirring while low supersaturated sample was treated at 65°C for 30 min under vigorous stirring. The slurry is filtered, washed thoroughly with distilled water and dried in an air oven at 110°C overnight. The samples were characterized by various physicochemical techniques whose experimental details are disclosed elsewhere [12]. Since physicochemical studies of some of the catalysts are disclosed in our earlier publications [13], focus will be made to study the effect of preparation methodology on the physicochemical properties of the samples.

The kinetics of the reaction was performed in an all glass recirculatory static reactor. About 1 g of powdered hydrotalcite-like compound (∼100 mesh size) was packed between silica wool plug. The glass beads occupying the void space served as a pre-heating zone for the reactant gas. The catalyst tube was radiatively heated by a tubular furnace whose temperature was controlled with an accuracy of ±1°C. Before each kinetic run, the precursor was evacuated 'in situ' at 350°C for 5 h to a final pressure of 5×10^{-6} Torr. It was then cooled to the reaction temperature and treated with 100 Torr of oxygen for 12 h to attain surface saturation. In other words, an equilibrium of oxygen exist between the catalyst surface and gas phase. The gas phase and weakly adsorbed oxygen were then removed by mild evacuation using a rotary pump for 2 min. A catalyst thus undergone these treatments was termed 'pretreated'. These pre-treatments are indeed necessary for the generation of a reproducible active surface [14]. It may be noted here that the hydrotalcite-like compound is only a precursor while the mixed metal oxide generated upon thermal activation is the true catalyst. 50 Torr of nitrous oxide (>99.5% purity) was admitted on to this pretreated catalyst from a gas reservoir (under circulation using a gas circulation pump) and the progress of the reaction was monitored by measuring the change in the total pressure of the system through a cathetometer capable of reading to an accuracy of ±0.001 cm. Reactions were usually followed for a period of 1 h and data were taken till reproducible results were obtained. For kinetic study, the conversion (of N_2O into N_2 and O_2) was restricted to 25%, in order to avoid diffusional limitations. No significant difference in the rates measured when the decomposition reaction was performed at different gas circulation speeds confirming the above statement.

The spent catalysts were analyzed using X-ray photoelectron spectroscopy (XPS) to perceive the surface nature and concentration of the active species. The spectra were recorded in an ESCALAB Mark II spectrometer (Vacuum Generators, UK) using MgKα radiation ($h\nu$ = 1253.6 eV) with a constant pass energy of 50 eV. The samples were mounted on a nickel holder in a pellet form and the working pressure in the analysis chamber was maintained below 5×10^{-9} mbar. Charging effects were corrected by referencing C 1*s* measurements at 285.0 eV. Ar^+ ion sputtering was done at 5×10^{-6} mbar pressure with a beam voltage at the order of 8 kV and a filament current of 30 μA cm^{-2}. The data were collected as an average of 10 scans of 40 s each and processed in a Apple Europlus microcomputer (USA). The binding energies were calculated using Al 2*p* line at 74.5 eV as an internal reference. It is well documented in literature that the binding energy calculations are more accurate with Al 2*p* line as reference for Al-containing samples [15].

3. Results and discussion

3.1. Physicochemical characterization of fresh and calcined samples

X-ray diffraction (XRD) of all the samples showed, within the composition range mentioned and irrespective of method of preparation, a single phase with hydrotalcite structure (JCPDS: 41-1428) exhibiting

Table 1
The cell parameters and surface area of the samples synthesised

Sample	M^{2+}/M^{3+} (atomic ratio)	*a* (Å)	*c* (Å)	*V* (Å^3)	Surface area (m^2/g)
CoAl2.0 : 1-HT(LS)	2.0	3.052	22.144	178.6	64
CoAl2.5 : 1-HT(LS)	2.6	3.055	23.057	186.4	57
CoA13.0 : 1-HT(LS)	3.0	3.059	23.578	191.1	35
CoAl2.0 : 1-HT(SP)	2.0	3.073	22.782	186.3	65
CoAl2.5 : 1-HT(SP)	2.6	3.081	23.758	187.1	28
CoAl3.0 : 1-HT(SP)	3.0	3.095	22.751	188.7	69

sharp and symmetric reflections for (0 0 3), (0 0 6), (1 1 0) and (1 1 3) planes and broad asymmetric peaks for (1 0 2), (1 0 5) and (1 0 8) planes, which are characteristic of these materials [13]. However, the samples prepared by low supersaturation technique yielded a better crystallinity over their corresponding sequentially precipitated samples. The lattice parameters were calculated by indexing the peaks under hexagonal crystal system and are summarized in Table 1. From the data presented, clearly with an increase in Co/Al atomic ratio both the lattice parameters '*a*' and '*c*' increased, The increase in the lattice parameter '*a*' can be attributed to higher octahedral ionic radius of Co^{2+} (0.74 Å) with respect to Al^{3+} (0.53 Å) while the increase in '*c*' parameter is due to a decrease in electrostatic interaction prevailing between layer and the interlayer [16]. Aging of LS samples at 65°C for 30 min was sufficient as there was no significant difference between the background corrected intensities of (0 0 6) and (1 1 0) XRD reflections and surface area of this sample and that of 24 h aged sample.

Transmission electron microscopy (TEM) showed a spherical to hexagonal morphology for LS prepared samples while a platy morphology for sequentially precipitated samples, indicating the effect of method of preparation. Energy dispersive X-ray analysis (EDAX) has been carried out to assess the homogeneity of the samples by monitoring the atomic composition at the microscopic level. The atomic composition was calculated based on the background subtracted integral intensity of the respective elemental peaks. Two regions with 25 and 50 nm spot sizes were examined to calculate the elemental composition for the sample CoAl3.0 : l-HT(LS), which showed a Co/Al atomic ratio of 3.0 assenting the sample homogeneity.

FT–IR absorption spectra of all the samples, irrespective of method of preparation, showed prominent bands around 3400, 1640 and 1370 cm^{-1} attributed to ν_{OH} stretching, ν_{OH} bending and ν_3 asymmetric stretching of carbonate, respectively. The low value of ν_{OH} in comparison with free hydroxide group (>3650 cm^{-1}) indicates that all hydroxyl groups of the sheets are hydrogen bonded. A weak absorption band around 3050 cm^{-1} was observed and is attributed to the hydrogen bonded interaction between water molecules' with carbonate ion present in the interlayer [17]. The other characteristic bands of carbonate, namely ν_2(out of plane deformation) and ν_4(in plane bending of carbonate) were observed around 870 and 680 cm^{-1}, respectively. A regular deviation exists between the observed vibrations of carbonate and free carbonate, which may be attributed to spatial confinement and hydrogen−bonded interaction of carbonate anion in the interlamellar space The other bands noticed in the region 1000–400 cm^{-1} were assigned to lattice vibrations such as Co–O(H)–Al bending and Co(Al)–O stretching. Further, the ν_{OH} band position for aged sample showed a red shift (shift to higher wave numbers) with an increase in Co/Al atomic composition, could be attributed to a decrease in the electrostatic interaction between layer and interlayer with its consequent effect on hydrogen bonding.

Thermogravimetric (TG) studies showed a two stage weight loss pattern for all the samples. The first weight loss occurred below 200°C and is attributed to the removal of interlayer water molecules. The second weight loss observed in the temperature range 250–300°C is associated with the removal of water from brucite-like sheet and CO_2 from the interlayer carbonate anion leading to the destruction of layered structure, with concomitant phase transformation of HT-like phase to spinel phase. The TG peak temperatures shifted to higher side while the net weight loss increased with a decrease in Co/Al atomic composition. In other words, an increase in aluminum content

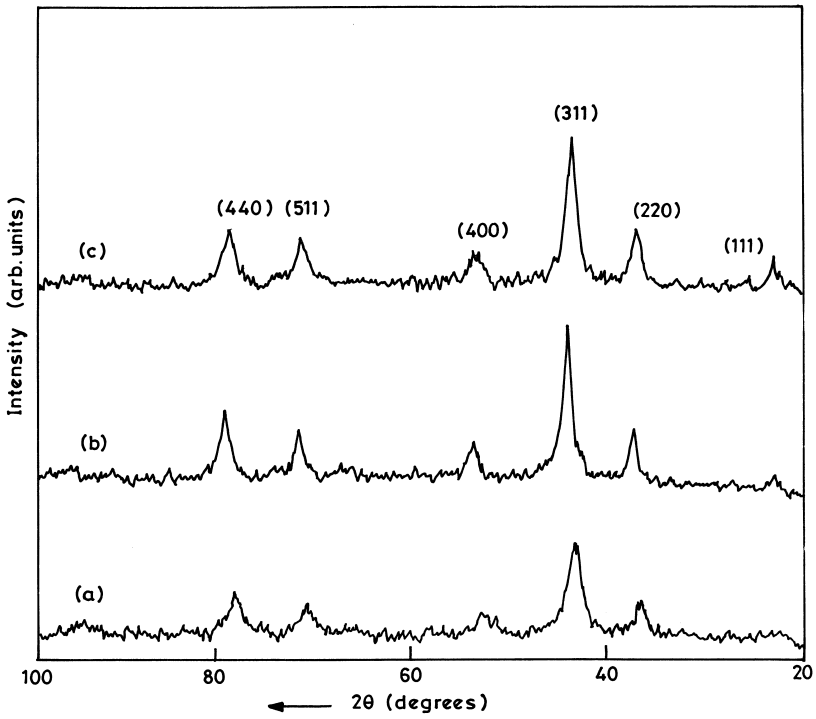

Fig. 1. XRD patterns of (a) CoAl2.0 : 1-HT(SP), (b) CoAl2.5 : 1-HT(SP), (c) CoAl3.0 : 1-HT(SP) calcined at 400°C for 5 h.

of the sheets enhances the electrostatic interaction between layer and the interlayer and thereby enhancing the thermal stability. Further, more carbonate is required for charge compensation and hence higher weight loss is noticed. TG transformation temperatures of corresponding LS and SP aged samples were similar indicating that the thermal stability is not significantly altered with method of preparation. DSC results documented TG results, by exhibiting two endothermic peaks corresponding to two weight losses.

Calcination of the materials was carried out to obtain a better picture on the nature of the thermally decomposed products (CHT — calcined hydrotalcite). Fig. 1 shows XRD pattern of aged samples, synthesized by sequential precipitation, calcined at 400°C for 5 h in air. All samples yielded a spinel phase upon calcination (probably a solid solution of Co_3O_4), however the crystallinity of the phase varied with Co/Al atomic composition. The formation of spinel at such low temperature (even at 200°C) is due to the facile oxidizability of Co^{2+} ion and the thermodynamic stability of Co_3O_4 (than CoO) in air

Table 2
Lattice parameters and surface area of $CoAlCO_3$-HTs aged samples calcined at 400°C for 24 h

Compound	*a* (Å)	Surface area (m^2/g)
CoAl2.0 : 1-HT(LS)	8.028	122
CoAl2.5 : 1-HT(LS)	7.989	145
CoA13.0 : 1-HT(LS)	7.995	143
CoAl2.0 : 1-HT(SP)	8.052	138
CoAl2.5 : 1-HT(SP)	7.965	134
CoAl3.0 : 1-HT(SP)	7.981	115
$CoAl_2O_4$	8.104	44–l60[a]
Co_2AlO_4	8.086	38–814[a]
Co_3O_4	8.084	43–1003[a]

[a] JCPDS file.

[18]. The lattice parameter '*a*' and surface area of the calcined samples (both LS and SP) are summarized in Table 2. The lattice parameters of pure $CoAl_2O_4$, Co_3O_4 and Co_2AlO_4 are also included in Table 2 for reference. It is clear that these values are much lower than that for pure cobalt oxides and cobalt aluminum oxides indicating the presence non-stoichiometry, probably in the form of anion vacancies and/or

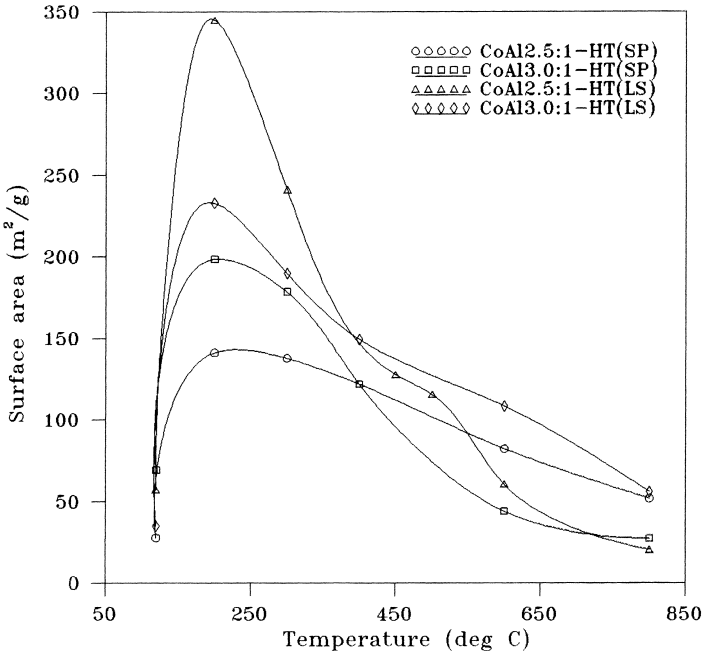

Fig. 2. Variation of surface area with calcination temperature for Co–Al HT-like compounds.

dissolution of Al^{3+} ions in spinel phase. The decrease in the lattice parameter '*a*' with an increase in Co/Al atomic ratio (CoAl2.0 : 1-CHT(SP) = 8.053 Å, CoAl3.0 : 1-CHT(SP) = 7.981 Å) may be due to an increase in the concentration of such defect sites. However, the surface area values of the calcined materials, irrespective of method of preparation, were similar indicating their alike behavior towards growth of the spinel phase. An increase in the calcination temperature enhanced the crystallinity of the spinel, as evidenced from the increase in the intensity and sharpness of (3 1 1) reflection, probably due to growth of the spinel phase and sintering of the particles. These results are substantiated by surface area measurements (Fig. 2) of the samples calcined at various temperatures for 1 h. For all the compounds, an increase in the surface area was observed up to 200°C, at which a transformation of HT-like phase to spinel phase occur with concomitant loss of water and CO_2, which lead to an increase in the porosity of the material. Furthermore, the surface area of LS prepared samples were higher than the corresponding SP prepared samples for this transient phase. Reichie et al [19] has earlier attributed this increase to the formation of pores/craters (through TEM) on the surface of the material through which water molecules and CO_2 escapes and showed that 60% of sample surface area is due to the contribution from these fine pores. On further increase in the calcination temperature a drop in the surface area was observed, which could be attributed to growth of the spinel phase formation, probably involving redissolution of metal ions. However, at higher calcination temperature (>600°C), XRD showed a clear increase in the intensity and sharpness of (3 1 1) reflection of the spinel phase conforming the particle size growth (sintering of mixed metal oxide particles). The extent of drop in surface area with temperature is almost similar irrespective of the composition. FT–IR spectra of the calcined materials showed a pattern similar to spinel phase [20] exhibiting two bands around 670 and 568 cm^{-1} correspondingly attributed to ν_1 and ν_2 vibrations. The observed band positions of these materials closely resemble the band position of Co_3O_4(672 and 590 cm^{-1}). The shift in the $\nu_2$band position, characteristic of Co^{3+} in octahedral co-ordination, may be due to the dissolution of Al^{3+} and/or non-stoichiometry associated with spinel phase.

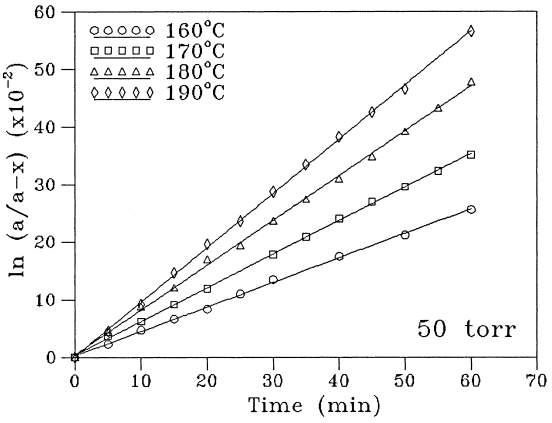

Fig. 3. Kinetic plots for the decomposition of N_2O on CoAl2.5 : 1-CHT(LS).

4. Kinetics and catalytic studies

At 50 Torr initial pressure of N_2O, all catalysts, irrespective of method of preparation or composition, exhibited a no inhibition by oxygen mechanism, i.e. the observed kinetic data can be fitted into a rate expression corresponding to first order condition Eq. (1). In other words,

$$-\mathrm{d}P/\mathrm{d}t = k_1 P_{\mathrm{N_2O}} \quad (1)$$

the adsorption and activation of N_2O molecule on the surface is the rate determining step [21] [1] . Fig. 3 shows a representative kinetic plot observed for CoAl2.5 : l-HT(LS) and the rate constants k: normalized per unit weight of precursor and k_{Co}: normalized per active cobalt ion present on the surface) measured at various temperatures over the catalysts are summarized in Table 3. The activation energy (E_a) and frequency factor ($\ln A$), also given in Table 3, were computed by constructing the Arrhenius plots. Fig. 4 shows a bar diagram indicating the temperature required for 25% conversion of N_2O over these catalysts.

[1] However, when the reaction was performed at 200 Torr initial pressure of N_2O, some of the catalysts showed a strong inhibition by oxygen (order with respect to oxygen was −0.5). Further, our activity studies under flow conditions also exhibited a strong reduction in N_2O conversion when the reaction was performed in an added oxygen containing feed stream. However, at 50 Torr and under our experimental conditions, owing to concentration of surface valence states and oxygen formed, the reaction rates were not significantly affected by oxygen.

It is clear from Fig. 4 that the activity increased with an increase in Co/Al bulk atomic composition. However, a little difference in the activity was observed between CoAl2.5 : 1-HT(LS) and CoAl3.0 : 1-HT(LS). This can further be substantiated by observing the rate constants for this series of catalysts measured at fixed temperature. For example, 'k' measured at 180°C on CoAl2.0 : 1-HT(LS), CoAl2.5 : l-HT(LS) and CoAl3.0 : l-HT(LS) are 5.94×10^{-3}, 7.94×10^{-3} and $8.00 \times 10^{-3}\,\mathrm{min}^{-1}$, respectively, confirming the above conclusion. These results could clearly imply that the number of adsorption centers increases with an increase in Co/Al bulk composition. It is apparent from the temperature range studied (150–280°C) that the activity arises primarily due to cobalt. However, comparison of normalized activity ($k_{\mathrm{Co}} = k/x_{\mathrm{Co}}$ where x_{Co} is the surface concentration of cobalt in fresh sample determined by XPS) of LS prepared catalysts showed a characteristic behavior wherein the intrinsic activity of cobalt increased with an increase in dilution. This is a normal trend observed for dilute solid solutions (0.05–5% of metal ion on a matrix) for N_2O decomposition [21].

Cobalt containing catalysts on various supports have been tried earlier for catalytic decomposition of N_2O [22]. The observed high activity of our catalysts prompted us to compare their activities with some of the similar catalysts reported. Cimino and Pepe [23] have carried out decomposition studies under static conditions (similar to our studies) over CoO–MgO solid solutions. They have concluded that the activity per cobalt ion increased with dilution, attributed on the basis of Co–O bond strength. However, comparing the activity of these catalysts with our catalysts based on the normalized rate constants indicated, k_{Co} of 0.05 at.% of CoO on MgO and 50 at.% CoO–MgO are 5×10^{-2} at 310°C and 4.0×10^{-4} at 375°C, respectively, while k_{Co} of CoAl3.0 : 1 HT(LS) is 2.3×10^{-2} at 190°C, that our catalysts are remarkably active. The most interesting feature of our catalysts is, despite the presence of high concentration of active metal ion (66–75 atoms of Co for every 100 atoms), the normalized activity was higher than dilute solid solutions. Comparison with CoO supported $A1_2O_3$catalyst (10% by wt.), however under flow conditions, also insinuated a superior behavior of our catalysts [24]. CoAl3.0 : l-HT(LS) exhibited 84% conversion of N_2O while CoO–Al_2O_3 showed

Table 3
Kinetic parameters for the decomposition of N_2O on CoAl-CHTs at 50 Torr

Compound	Temperature (°C)	k (min^{-1}) ($\times 10^{-3}$)[a,b]	k_{Co} ($\times 10^{-2}$)[c] (min^{-1})	E_a ($kJ\,mol^{-1}$)	$\ln A$ (min^{-1})	Conversion at 30 min time interval (%)
CoAl2.0 : 1-HT(LS)	170	4.663	1.793	28.1	2.2	12.8
	180	5.942	2.285			15.6
	190	6.359	2.445			18.4
	200	7.500	2.885			20.3
CoAl2.5 : l-HT(LS)	160	4.414	1.193	43.5	6.7	12.6
	170	5.949	1.608			16.2
	180	7.938	2.145			21.0
	190	9.737	2.632			25.0
CoAl3.0 : l-HT(LS)	160	5.077	1.209	35.9	4.7	14.4
	170	6.375	1.518			17.8
	180	8.000	1.905			21.3
	190	9.629	2. 293			25.4
CoAl2.0 : 1-HT(SP)	250	9.330		39.3	4.3	24.6
	260	10.770	ND[d]			27.2
	270	13.160				30.0
	280	15.150				36.0
CoAl2.5 : 1-HT(SP)	190	4.896		35.1	3.8	13.8
	210	6.923				19.4
	230	10.230	ND			26.4
	250	13.840				33.6
CoAl3.0:1-1-IT(SP)	150	3.652		46.8	7.4	10.4
	160	5.000				13.8
	170	6.473	ND			17.0
	180	7.878				21.0

[a] All catalysts obeyed no inhibition by oxygen mechanism.
[b] Normalised rate constant per unit gram of precursor.
[c] Normalised rate constant per active cobalt ion $k_{Co} = k/x_{Co}$ where x_{Co} is the surface concentration of cobalt in fresh sample determined by XPS.
[d] Not determined.

only 15% conversion at 450°C under similar reaction conditions (985 ppm of N_2O in He, 0.1 g sample and flow rate is l00 cm^3/min.). These results imply that, although Co^{2+} is the active species in all catalysts, the environment around Co^{2+} (imposed by matrix), the surface structure and composition and preparation methodology play a crucial role in controlling the overall activity [25]. We believe that, owing to the high concentration of cobalt in our catalysts, it is not possible to have isolated Co^{2+} centers on the surface where participation of neighboring ions has to be considered. In our case, one can visualize a system comprising Co^{2+}–O–Co^{3+} may constitute an active site and such kind of system is rationalized by Zener double exchange which lead to an average and easily adaptable oxidation state that facilitates both adsorption and desorption processes [26].

Comparison of the activity of the catalysts synthesized by different preparation methods indicated that Co–Al catalysts synthesized under LS conditions are correspondingly more active than those prepared under SP conditions (k at 190°C; CoAl2.5 : l-HT(LS) = 9.74×10^{-3}, CoAl2.5 : 1-HT (SP) = 4.90×10^{-3}; k at 180°C CoAl3.0 : l-HT(LS) = $8.00 \times l0^{-3}$, CoAl3.0 : l-HT(SP) = 7.88×10^{-3}). The observed difference in the activity could be due to a higher concentration of the active species on the surface of the catalysts prepared under LS conditions. Further, it is clear that the difference in the activity between the two series of catalysts decreases with an

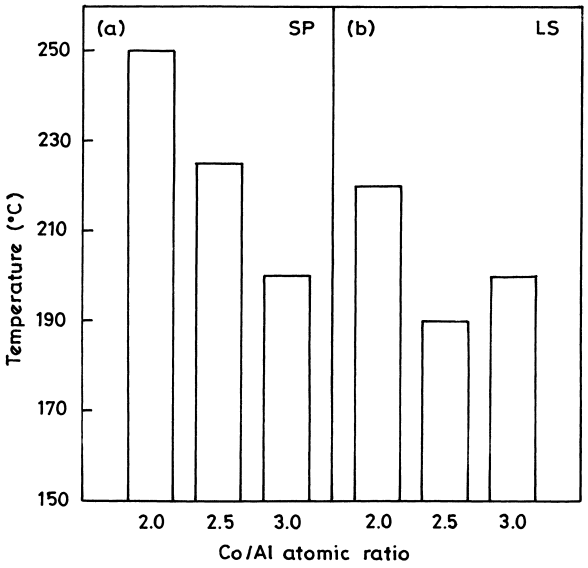

Fig. 4. Temperature required for 25% conversion of N_2O over CoAl-CHTs with various compositions (a) Sequential precipitation, (b) Low supersaturation.

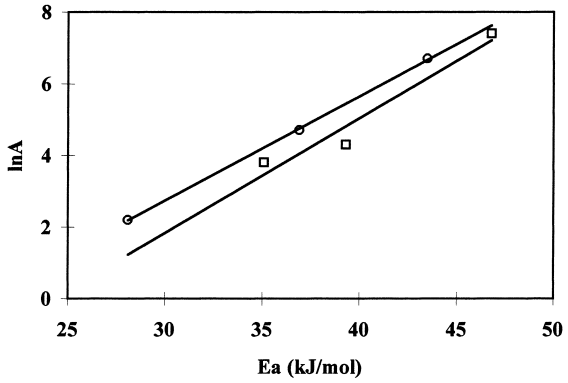

Fig. 5. Compensation plots for the decomposition of N_2O on CoAl-CHTs (□) CoAl-CHT(SP); (○) CoAl-CHT(LS).

Table 4
Lattice parameters and surface area of spent catalysts

Compound	a (Å)	Surface area (m^2/g)
CoAl2.0 : 1-HT(LS)	8.032	97
CoAl2.5 : 1-HT(LS)	8.036	62
CoAl3.0 : 1-HT(LS)	8.062	83
CoAl2.0 : 1-HT(SP)	8.056	53
CoAl2.5 : 1-HT(SP)	8.085	48
CoAl3.0 : 1-HT(SP)	8.035	61

increase in cobalt content. In other words, preparation methodology have significant influence for the sample having low Co/Al atomic composition. Since the activation energies for the corresponding catalysts are almost similar (8–l0 kJ/mol), the activity difference between these two series of catalysts, is probably due to the differences in the extent of segregation of active species on the surface. Further, on both the series of catalysts, a linear correlation was observed between E_a and $\ln A$ (Fig. 5) suggesting the operation of compensation effect. This would imply that although cobalt is the active species on all the catalysts, the energetics of the active sites are significantly modified by their associated environment, denoting the heterogeneity of these sites [26]. XRD analysis of the spent catalysts showed a spinel phase with varying crystallinity depending on the Co/Al atomic composition and synthesis methodology, with non-stoichiometry, as evidenced from their lattice parameter values (along with their surface areas), furnished in Table 4.

Considering reaction mechanism, in the case of thermally calcined Co-containing HT-like compounds, the adsorption of N_2O occurs on Co^{2+} site where a partial donation of electron from its filled *d*-orbital to π^* molecular orbital of N_2O (in the case of 50 Torr) occur thereby gets oxidized to $Co^{(2+\delta)+}$. Due to the instability of $N_2O_{ads}{}^{\delta-}$, it decomposes rapidly with an evolution of N_2 and adsorbed $O^{\delta-}$ The adsorbed $O^{\delta-}$ species migrates on the surface, where matrix effects play a predominant role, and desorb as molecular oxygen through combination of two such species concomitantly donating electrons back to $Co^{(2+\delta)+}$ [22]. Thus, the concentration of Co^{2+} present on the surface controls the overall rate. Hence, the differences observed in the activity of these catalysts could be rationalized on the basis of the variation in the surface concentration of Co^{2+}.

4.1. Surface studies of spent catalysts (LS samples) by X-ray photoelectron spectroscopy

It is well known, that the nature of the active species present on the surface of the catalyst plays a predominant role in determining the activity of the reaction [15]. X-ray photoelectron spectroscopy (XPS) has been carried out for the spent catalysts (N_2O treated catalyst) in order to characterize the species present on the surface. The etching of the surface

Table 5
Salient features of XP spectra of CoAl-CHTs(LS) spent catalysts (Reference — Al 2*p* line)

Region	CoAl2.0 : 1-HT(LS)	CoAl2.5 : 1-A(LS)	CoAl3.0 : 1HT(LS)
Co $2p_{3/2}$ satellite	783.4	782.0	783.4
Co $2p_{1/2}$ satellite	798.4	797.0	798.4
DE (Co $2p_{3/2}$–Co $2p_{1/2}$)	15.0	15.0	15.0
O 1*s*	533.0	532.5	532.9
Al 2*s*	119.5	119.4	119.4
Co/Al atomic ratio	0.36	0.59	0.73

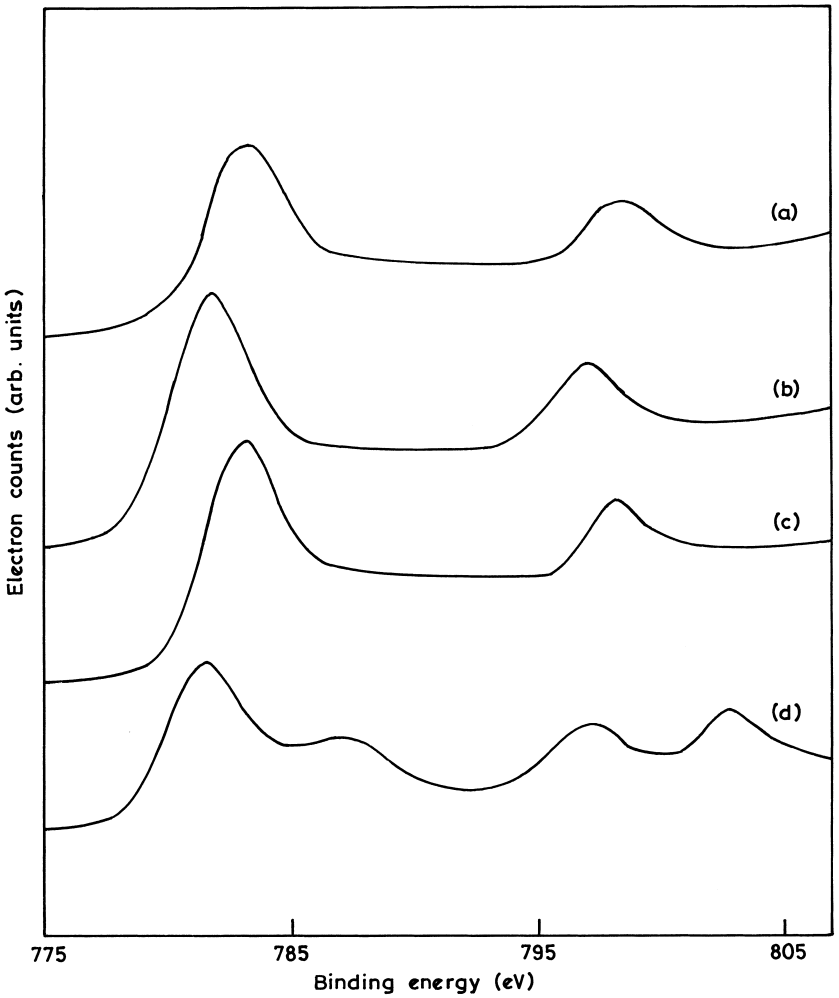

Fig. 6. XP (Co 2*p*) spectra of spent catalysts (a) CoAl2.0 : 1-HT(LS), (b) CoAl2.5 : 1-HT(LS), (c) CoA13.0 : 1-HT(LS), (d) $CoAl_2O_4$.

was performed using Ar^+ ion sputtering to study the reduced surface/sub-surface region.

The salient features of the XP-spectra are summarized in Table 5 and Co 2*p* spectra of these samples are shown in Fig. 6. For comparison purpose, XP spectrum of pure $CoAl_2O_4$ is also included. Surface composition of the catalysts is determined using the formula (Eq. (2)) reported by Powell and Larsson [27]

$$n_A/n_B = (I_A/I_B)(\sigma_A/\sigma_B)(E_B/E_A)^{1/2} \quad (2)$$

In our studies Co/Al surface composition is calculated using integrated intensity of Co $2p_{3/2}$ (with satellite) and Al 2*p* XPS peaks. The photo-ionization cross section (σ) for these elements are taken from literature [28]. The surface atomic composition (Co/Al) calculated for these spent catalysts are given in Table 5.

Focusing attention on Co 2*p* spectra, it is clear that the satellite contribution for Co $2p_{3/2}$ is negligible for spent catalysts indicating that cobalt is present predominantly in +3 oxidation state on the surface. It is well established in literature [29] that diamagnetic Co^{3+} (t_{2g}^6) does not possess any satellite features. Furthermore, the binding energy difference between Co $2p_{3/2}$ and Co $2p_{1/2}$ is around 15.0 eV confirming (spin-orbit splitting) the presence of Co^{3+} on the surface. This could probably be due to surface oxidation of Co^{2+} (thought to be the active species generated after activation of catalyst) to Co^{3+} during nitrous oxide decomposition reaction. However, the binding energy values calculated are slightly higher than those reported in the literature (~781.5 eV) [30]. This could due to a strong interaction of Co^{3+} on the surface, probably in the form of CoO(OH) species as the samples were synthesized as hydroxycarbonates through coprecipitation [25,31]. Further, Co $2p_{3/2}$ peak of these spent catalysts was broad and tailing (however Co 2*p* peak was sharp with prominent satellite features for $CoAl_2O_4$; Fig. 6) towards higher binding energy side which is similar to the spectra of Co_3O_4 [32]. Such tailing of this peak towards higher energy side along with the shift in binding energy was attributed to the presence of hydroxyl functionality in CoO–MgO catalysts [25]. It is also reported in literature [32] that segregation of Co_3O_4 is favorable with higher percentage loading of cobalt (>30%) in the case of cobalt supported alumina catalysts under oxidizing conditions. Hence, we presume the possible formation of Co_3O_4 on the surface during the decomposition reaction.

The O 1*s* peak of $CoAl_2O_4$ was sharp (FWHM = 2.7 eV) whose binding energy was observed at 530.8 eV, correspond to O^{2-} lattice oxygen. However, the O 1*s* peaks were relatively broad for spent catalysts, whose FWHM (~3.3 eV) showed a small variation with bulk composition and a tailing end indicating the presence of more than one kind of oxygen present on the surface. Further, a shift in the binding energy values to higher side was observed (with respect to $CoAl_2O_4$), occurring around 531.5 eV in most of the cases, could be assigned for oxygen of hydroxyl groups and/or non-stoichiometric spinel-type phases [25,30]. There is no considerable shift in Al 2*s* binding energy value centered around 119.5 ± 0.1 eV indicating the presence of Al^{3+} on the surface, less affected due to electronic interactions.

An important factor regarding the surface property of oxides is the occurrence of preferential segregation of one ion over other on the surface leading to a difference between the bulk and surface composition and in turn on catalytic properties. This could be explained based on the differences in the surface free energies of individual elements wherein the element which has a low surface free energy preferentially segregate to the surface [33]. It is clear from Table 5 that the surface Co/Al atomic composition is very much different from the bulk composition with a preference of aluminum segregating on the surface. For example, the bulk Co/Al atomic composition for CoAl3.0 : 1-HT(LS) is 3.0 while surface Co/Al atomic composition of the fresh sample is 0.72 and that of 10 min etched sample is 1.08. Al which has got low surface free energy ($\gamma_{Al} = 1140\,mJ/m^2$; $\gamma_{Co} = 2100\,mJ/m^2$; almost half the value of cobalt) has apparently segregated to the surface. Such surface enrichment of trivalent cation on the surface was earlier observed by Trifiro et al. [34] for Ni–Al hydrotalcites and Uzunova et al. [35] for Co–Fe hydrotalcites upon calcination.

Fig. 7 show the Co 2*p* XP spectra of spent catalysts etched for 1 and 10 min. This is done in order to discern the reduced surface/sub-surface level features which may be active surface participating in our catalytic reaction [30]. Interestingly, in all catalysts Co $2p_{3/2}$ showed a prominent satellite around 6 eV shifted from the main line position after Ar^+ sputtering (even after 1 mm). Furthermore, the intensity of the satellite peak (compare Fig. 7(a) and (d)) enhanced with an increase in etching time. This clearly indicates the generation of Co^{2+} on the surface upon sputtering. The binding energy value of Co $2p_{3/2}$ also showed a value between 781.5 and 782.8 eV, depending on the nature of the sample, which resembles the value of cobalt in +2 oxidation state, as evidenced by many bivalent cobalt compounds (~782.0 eV) [36]. The spin-orbit splitting between Co $2p_{3/2}$ and Co $2p_{1/2}$

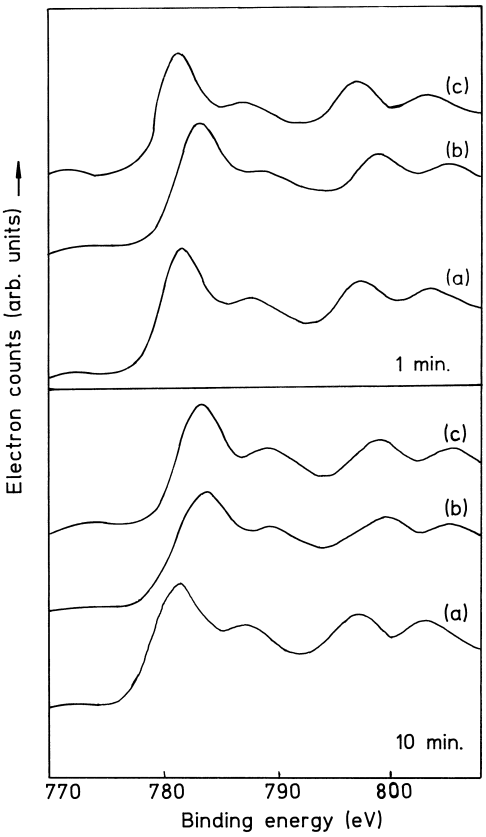

Fig. 7. XP (Co 2*p*) spectra of spent catalysts after 1 min Ar^+ and 10 min Ar^+ sputter etching (a) CoAl2.0 : 1-HT(LS), (b) CoAl2.5 : 1-HT(LS), (c) CoAl3.0 : 1-HT(LS).

showed a value >15.5 eV substantiating the presence of Co^{2+}. However, upon etching only a slight change in O 1*s* peak position and shape was observed indicating (FWHM of fresh and etched samples were almost same) the retention of the similar kind of oxygen on the reduced/sub-surface as that of fresh sample.

Surface composition analysis of etched samples, given in Table 6 indicated a surface enrichment of cobalt. The increase is nearly 70% in the case of CoAl2.0 : I -HT(LS). The enhancement in surface concentration decreases with an increase in the bulk composition [30% in the case of CoAl2.5 : l-HT(LS) and 20% in the case of CoAl3.0 : l-HT(LS)]. These differences observed in the extent of enrichment of cobalt on the surface could be due to differences in the availability of sites on the surface. We believe that a significant reduction and reconstruction of surface may occur during our pretreatment which generate an active surface (probably similar to the one generated after Ar^+ sputtering), which is involved in the catalytic reaction. A marked difference in the activity of N_2O decomposition between CoAl2.0 : l-HT(LS) and CoAl3 0 : 1 HT(LS) (see Fig. 4) could be related to higher surface concentration of cobalt for the later. However, similar activity observed between CoAl2.5 : l-HT(LS) and CoAl3.0 : l-HT(LS) (only 10° difference between these two catalysts for achieving nearly 25% conversion) may be due to the presence of similar surface concentration of cobalt. From these results, it may be possible to conclude that the high activity observed for our catalysts could be due to a good dispersion of Co^{2+} ion (generated by surface reduction and reconstruction) on a relatively large surface, probably in form of Co^{2+}–O–Co^{3+} redox couples, wherein the overall activity is controlled by the surface concentration of active metal ion while the intrinsic activity is controlled by the nature of cobalt present in the samples. Further, one cannot completely exclude the contribution of activity from defective structure of spinel, as evidenced from XRD and IR measurements.

5. Conclusions

1. In the composition range studied, irrespective of method of preparation, all the samples were crystallized in HT-like structure without any impurity. However, the crystallinity was affected with method of preparation and composition.
2. Thermal treatment of these materials yielded non-stoichiometric spinel phase (even at 200°C), whose crystallinity enhanced with an increase in calcination temperature.
3. All samples obeyed a first order kinetic equation indicating that the adsorption and activation of N_2O on the surface is rate controlling.
4. The activity of samples synthesized under LS conditions showed a better activity than the samples prepared by SP method.
5. The variation in the observed activity is in direct relation with the surface concentration of cobalt The normalized activity for nitrous oxide decomposition reaction increased with an increase in dilution.

Table 6
Surface and subsurface compositions of CoAl-CHTs(LS) spent catalysts

Parameters	CoAl2.0 : 1-HT(LS)	CoAl2.5 : 1 -HT(LS)	CoAl3.0 : 1-HT(LS)
Cobalt			
Bulk[a]	0.66	0.71	0.75
Fresh[b]	0.26	0.37	0.42
Etched (1 min)[b,c]	0.44	0.48	0.49
Etched (10 min)[b,c]	0.43	0.47	0.52
Aluminum			
Bulk[a]	0.33	0.29	0.25
Fresh[b]	0.74	0.63	0.58
Etched (1 min)[b,c]	0.56	0.52	0.51
Etched (l0 min)[b,c]	0.57	0.53	0.48
Co/Al atomic ratio			
Bulk[a]	2.0	2.5	3.0
Frcsh[b]	0.35	0.59	0.72
Etched (1 min)[b,c]	0.79	0.92	0.96
Etched (10 min)[b,c]	0.75	0.89	1.08

[a] Determined using inductively coupled plasma emission spectroscopy.
[b] Determined using XPS.
[c] Ar^+ sputtering.

Acknowledgements

S.K thanks Dr. R.V. Jasra, Deputy Director, CSMCRI, Bhavnagar and Dr S.D. Gomkale, Acting Director, CSMCRI, Bhavnagar for helpful discussions. We thank all reviewers for their constructive criticism and valuable suggestions, which definitely helped us to improve the quality of our manuscript significantly. We also thank Air Products and Chemicals Inc., Allentown, USA, for financial assistance and M/s Engelhard Corporation, USA for permitting us to present this work.

References

[1] S.S. Cliff, M.H. Thiemens, Sci. 278 (1997) 1774.
[2] C.S. Swamy, S. Kannan, S. Velu, in: V.G. Kumar Das (Ed.), Main Group Elements and their Compounds, Narosa Publishing House, New Delhi, India, 1996, p. 112.
[3] F. Cavani, F. Trifiro, A. Vaccari, Catal. Today 11 (1991) 173.
[4] W.T. Reichle, J. Catal. 94 (1985) 547.
[5] F. Trifiro, A.Vaccari, in: R.K. Graselli, A.W. Sleight (Eds.), Structure-Activity and Selectivity Relationships in Heterogeneous Catalysis, Elsevier, Amsterdam, 1991, p. 157.
[6] M.J. Climent, A. Corma, S. Iborra, J. Primo, J. Catal 151 (1995) 60.
[7] S. Kannan, C.S. Swamy, Y. Li, J.N. Armor, T.A. Braymer, US Patent 5, 407,652, 1995.
[8] S. Velu, C.S. Swamy, Catal. Lett. 40 (1996) 265.
[9] A. Guida, M.H. Lhouty, D. Tichit, F. Figueras, P. Geneste, Appl. Catal. A 164 (1997) 251.
[10] P.S. Kumbhar, J. Sanchez-Valente, F. Figueras, J. Chem. Soc. Chem. Commun. (1998) 1092.
[11] S. Kannan, C.S. Swamy, Appl. Catal. B 3 (1994) 109.
[12] S. Kannan, C.S. Swamy, J. Mater. Sci. 31 (1996) 2353.
[13] S. Kannan, C.S. Swamy, J. Mater. Sci. 32 (1997) 1623.
[14] J. Christopher, C.S. Swamy, J. Mol. Catal. 62 (1990) 69.
[15] B.R. Strohmier, D.E. Leyden, R. Scott Field, D.M. Hercules, J. Catal. 94 (1985) 514.
[16] O. Clause, M. Goncalves Coelho, M. Gazzano, D. Matteuzzi, F. Trifiro, A. Vaccari, Catal. Today 8 (1993) 169.
[17] F.M. Labojos, V. Rives, M.A. Ulibarri, J. Mater. Sci. 27 (1992) 1546.
[18] T. Sato, U. Fujita, T. Endo, M. Shimada, A. Tsunashima, Reactivity of Solids 5 (1988) 219.
[19] W.T. Reichle, S.Y. Kang, D.S. Everhardt, J. Catal. 101 (1986) 352.
[20] J. Preudhomme, P. Tarte, Spectrochim. Acta 27A (1971) 1817.
[21] A. Cimino, La Chimica e Ia Industria, 56 (1974) 27.
[22] F. Kapteijn, J. Rodriguez-Mirasol, J.A. Moulin, Appl. Catal. B 9 (1996) 25.
[23] A. Cimino, F. Pepe, J. Catal. 25 (1972) 362.
[24] J.N. Armor, T.A. Braymer, T.S. Farris, Y. Li, F.P. Petrocelli, E.L. Weist, S. Kannan, C.S. Swamy, Appl. Catal. B 7 (1996) 397.
[25] R.S. Drago, K. Jurczyk, N. Kob, Appl. Catal. B 13 (1997) 69.
[26] R. Larsson, Catal. Today 4 (1989) 235.
[27] C.J. Powell, P.E. Larson, Appl. Surf. Sci. 1 (1978) 186.
[28] J.H. Scofield, J. Electron Spectrosc. Rel. Phenomenon 9 (1976) 129.

[29] R.I. Declerck-Grimme, P. Canesson, R.M. Friedman, J.J. Fripat, J. Phys. Chem. 82 (1978) 885.
[30] T.J. Chuang, C.R. Brundle, D.W. Rice, Surf Sci. 59 (1976) 413.
[31] N. Okazaki, Y. Yamamoto, H. Itoh, A. Tada, Chem. Lett. (1998) 807.
[32] R.L. Chin, D.M. Hercules, J. Phys. Chem. 86 (1982) 360.
[33] A.R. Miedema, Z. Metallakunde 69 (1978) 287.
[34] F. Tirfiro, A. Vaccari, O. Clause, Catal. Today 21 (1994) 185.
[35] E Uzunova, E.D. Klissurski, I. Mitov, P. Stefanov, Chem. Mater. 5 (1993) 576.
[36] N.S. Mclntyre, M.G. Cook, Anal Chem. 47 (1975) 2208.